



Technical note

Load-settlement characteristics of large-scale square footing on sand reinforced with opening geocell reinforcement

A. Shadmand^a, M. Ghazavi^{b,*}, N. Ganjian^a^a Department of Civil Engineering, Science and Research Branch, Islamic Azad University, Tehran, Iran^b Department of Civil Engineering, K.N. Toosi University of Technology, Tehran, Iran

ARTICLE INFO

Keywords:

Geosynthetics
Geocell with an opening
Large scale model test
Reinforced sand
Square footing
Surface deformation
Improvement factor

ABSTRACT

This paper describes load-carrying characteristics of a series of large-scale steel square footing tests performed on sand reinforced with two types of reinforcement methods. These are full geocell reinforcement (FGR) and geocell with an opening reinforcement (GOR). A thick steel square plate with 500 mm by 500 mm dimensions and 30 mm thickness was used as foundation. The parameters varying in the tests include the depth of geocell mattress (u), width of opening in geocell in the GOR type (w), relative density of sand (D_r) and number of geocell layers (N). The results revealed that the use of GOR and FGR methods enhances significantly the footing load carrying capacity, decreases the footing settlement and decreases the surface heave. It has been found that the use of GOR with an opening width of $w/B < 0.92$, has the same improvement effect on the footing load-carrying response as the FGR has (B = footing width). Furthermore, with increasing the number of geocell layers from 1 to 2 in both GOR and FGR methods, the footing bearing pressure increases and footing settlement, surface heave and difference of performance between FGR and GOR mattress decrease.

1. Introduction

Geosynthetic materials have been used in practice due to their costs, performance, tensile resistance, durability and ease of application for e.g., construction of footing over soft soil, embankments, road construction and in general for improvement of weak ground supporting variety constructions. The behavior of geosynthetic reinforcement has been investigated extensively (Binquet and Lee, 1975; Khing et al., 1993; Dash et al., 2001a,b,2007, Dash, 2012; Yoon et al., 2004; Ghosh et al., 2005; Chung and Cascante, 2007; El Sawwaf, 2007; Sharma et al., 2009; Latha and Somwanshi, 2009; Boushehrian et al., 2011; Lavasan and Ghazavi, 2012; Lavasan et al., 2017; Koerner, 2012; Chen et al., 2013; Demir et al., 2013; Badakhshan and Noorzad, 2017; Shahin et al., 2017).

Over recent last decades, many investigators have confirmed the benefits of planar reinforcement on enhancement of load-carrying characteristics of footings. Binquet and Lee (1975), Fragaszy and Lawton (1984), Khing et al. (1993), Hataf et al. (2010), Demir et al. (2013) and Roy and Deb (2017) performed model tests to investigate such characteristics. Ghazavi and Lavasan (2008) and Lavasan and Ghazavi (2012) conducted tests to evaluate the behavior of two closely spaced footings on geogrid reinforcement. They reported that the influence of the interference on the settlement of closely spaced footings

at a given load decrease by increasing the number of geogrid layers. They also performed numerical analyses to evaluate the performance of footing on planar geosynthetic reinforcement.

In recent years, three dimensional geocell reinforcement has been used, resulting in better enhancement of footing, embankment and subballast load-carrying characteristics (Rea and Mitchell, 1978; Shimizu and Inui, 1990; Adams and Collin, 1997; Dash et al., 2001a,b,2003; Biswas et al., 2013; Biabani et al., 2016; Oliaei and Kouzegaran, 2017; Kargar and Mir Mohammad Hosseini, 2017). Dash et al. (2003, 2004) carried out model tests on circular footing supported by geocell reinforced soil overlying soft clay. Dash (2012) carried out tests to investigate the influence of geocell on load-carrying mechanism of strip footings. Sitharam and Hegde (2013) and Hegde and Sitharam (2015a, b, c, 2017) have conducted comprehensive numerical and experimental studies to evaluate the behavior of the footings on geocell with additional basal geogrid reinforced soil and bed reinforced with the bamboo cells. They showed that planar geogrid at the base of the geocell mattress enhanced the load carrying capacity significantly. Ngo et al. (2016) studied the load-deformation behavior of geocell-stabilized subballast subjected to cyclic loading using a novel track process simulation. The results indicated that the geocell decreased the vertical and lateral deformation of subballast assemblies at any given frequency.

* Corresponding author.

E-mail addresses: shadmand.a@abhariau.ac.ir (A. Shadmand), ghazavi_ma@kntu.ac.ir (M. Ghazavi), n.ganjian@srbiu.ac.ir (N. Ganjian).

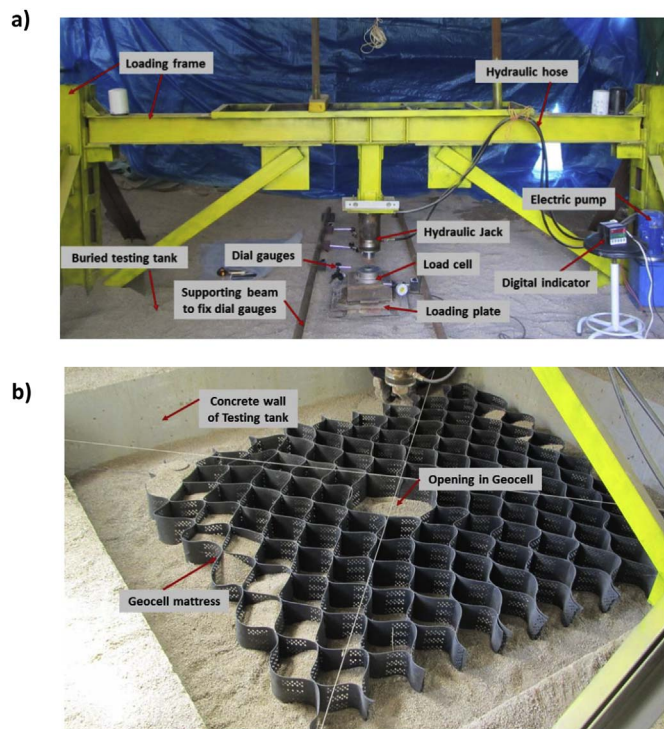


Fig. 1. Test setup: (a) General arrangement of test setup; (b) Test tank and geocell mattress.

In almost all past studies, the footing size has been small and results may not be applicable to large size footings especially when geocell is used as soil reinforcement. Adams and Collin (1997) conducted only one test on a 910 mm square plate placed beside six plates in a tank. They did not consider boundary effects and interaction effects of each footing on neighboring footings which is quite important, as stated by Lavasan and Ghazavi (2012). Thus, it is necessary to understand more comprehensively the behavior of larger scale footings on geocell-reinforced soil.

In the present study, a total number of 18 large-scale tests were performed using a thick square plate with 500 mm width and 30 mm thickness as footings supported by both unreinforced and geocell-reinforced sand. In this research, for the first-time, geocell with an opening reinforcement (GOR) was used as the bed for large steel square plate as footing. The current research has three strong features: 1) the use of large footing; 2) the use of GOR for the first time and 3) the use of geocell with dimensions close to real condition. For GOR type reinforcement, geocell layers were used around the footing bottom level which is named here as 'Geocell with an Opening Reinforcement' (GOR), as shown in Figs. 1b and 2b. To evaluate the performance of GOR, several large-scale tests were conducted on unreinforced sand and normally geocell reinforced which is called 'Full Geocell Reinforcement' (FGR), as shown in Fig. 2a. As will be shown, the GOR method can be an appropriate alternative to FGR method in cases where access to the footing bottom is difficult or limited. The various parameters studied in this research include the depth of the first geocell layer (u), the number of geocell layers (N), the width of opening in geocell reinforcement (w) and relative density of sand (D_r).

2. Large scale tests

A series of large scale model tests were conducted by a loading set up consisting of a rigid loading frame, test tank, loading system, steel plate as footing and load and settlement measuring devices. The general arrangement of the test setup is shown in Fig. 1. As seen, the loading frame supports a hydraulic jack and provides reaction loads to apply on

the footing. The loading frame was designed to deflect slightly under 250 kN maximum applied load. Some diagonal elements were used to control undesirable deflections of columns and foundation of loading frame.

The soil bed was prepared in a steel reinforced concrete test tank with inside dimensions of 3000 mm length, 3000 mm width and 2000 mm height. In order to reduce the boundary effects, the size of the test tank was in conformity with that used by Ueno et al. (1998). Also, a numerical model was applied for this purpose. The sidewall friction effects on the model test results were reduced by coating the inside of the walls with petroleum jelly. The test tank was built underground. This facilitates easily to fill and evacuate sand in the tank due to large size of the tank (Fig. 1).

The load is applied on the footing using a hydraulic jack that has a maximum stroke of 15 cm and 220 kN maximum load. The loading steel plate was square with 500 mm width and 30 mm thickness. To provide enough flexural rigidity for the footing, two identical plates with dimensions of 500 mm × 500 mm × 30 mm were welded together. To prepare a rough surface for the footing bottom, coarse sand paper was adhered to the plate.

The loading shaft was tipped to a half-sphere shape sitting mounted on the load cell. This zone was completely lubricated with grease to decrease the friction on the surface as much as possible. The load was applied on the footing while it remained vertical during tests to prevent the footing from tilting.

To measure the settlement of the footing, three dial gauges with an accuracy of 0.01% of full range (100 mm) were attached to two reference beams and their tips were placed about 10 mm inwards from the edge of the plate, as shown with DG1, DG2 and DG3 in Fig. 2c. In addition, to measure heave or settlement of the soil surface at points 1.5B and 2.5B (B = footing width) to the either side of the footing center, four dial gauges were used as represented by DG4, DG5, DG6 and DG7 in Fig. 2c. A compression load cell with an accuracy of $\pm 0.02\%$ full-scale was placed between the loading shaft and center of the footing plate.

3. Test materials

3.1. Sand

The sand classified as SP in the Unified Soil Classification System (USCS) is relatively uniform silica with grain size ranging 0.08–10 mm. To have negligible size effect, according to Kusakabe (1995), the sand grain size is small enough than the footing width ($\frac{B}{D_{50}} > 50 \sim 100$). The friction angles of the sand at two relative densities were determined using drained triaxial compression tests. The sand properties are shown in Table 1.

3.2. Geocell reinforcement

In the past research work, geocell was fabricated in two methods. In the first method, geocell mattresses are prepared by cutting geogrid to required lengths and heights from full rolls and placing them in transverse and diagonal directions on the soil bed with bodkin joints (plastic strips) inserted at connections (Bush et al., 1990). In the second method, geocell is made of a type of planar geotextile thermo-welded to form a honeycomb structure with an open top and bottom. In the current research, due to having large footing size, none of two methods has been used and instead, to achieve uniformity in reinforcement, prefabricated factory produced geocell was used. The pocket size of geocell (d) is taken as the diameter of an equivalent circular area of the pocket opening (A_g). In all tests, the pocket size of the geocell (d), the height of the geocell layer (H) and the width of the geocell layer (b) were kept 220, 150 and 2500 mm, respectively. Thus d/B , H/B , and b/B were considered 0.44, 0.3 and 5, respectively.

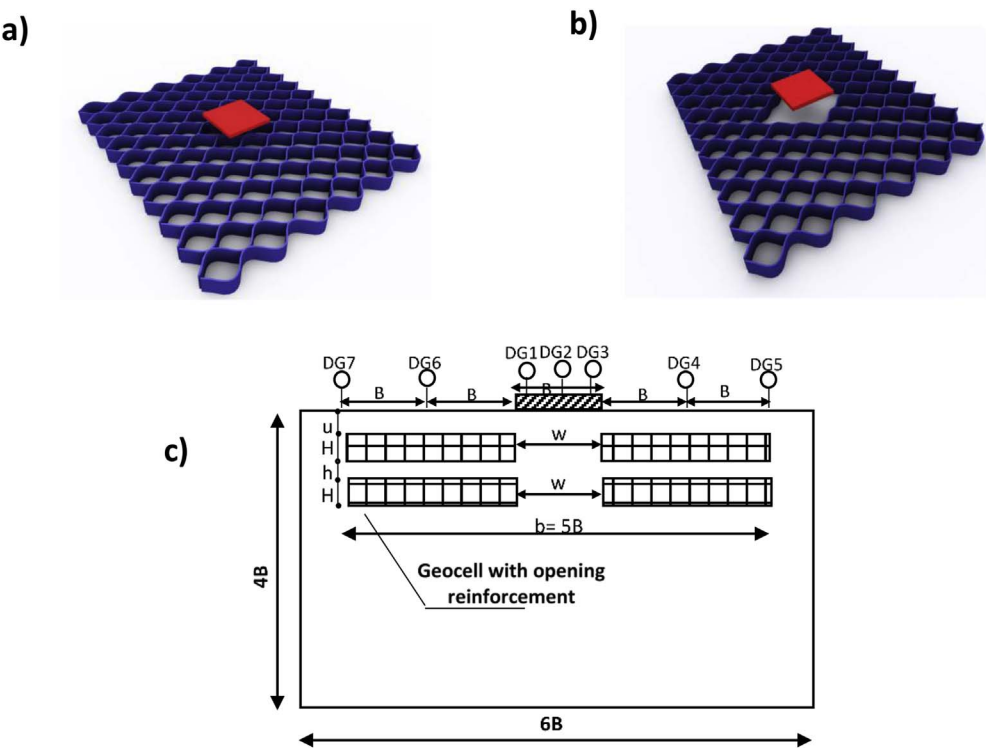


Fig. 2. Schematic view of geocell reinforcement, (a) FGR; (b) GOR; (c) contributing parameters for square footing and geocell arrangement.

Table 1
Properties of sand used in current tests.

Value	Parameter
1.2	Effective particle size, D_{10} (mm)
2.1	D_{30} (mm)
2.9	Mean particle size, D_{50} (mm)
3.2	D_{60} (mm)
2.7	Uniformity coefficient, C_u
1.15	Curvature coefficient, C_c
15.1	Minimum dry unit weight, γ_{dmin} (kN/m ³)
18.6	Maximum dry unit weight, γ_{dmax} (kN/m ³)
38°	Friction angle at $D_r = 35\%$
41°	Friction angle at $D_r = 65\%$

Table 2
Geometrical and engineering properties of geocell used in current tests (Geoplas data sheet).

Value	Description
Polymeric nano-composite alloy	Material
Perforated	Cell wall surface
15	Yield tensile strength (kN/m)
29	Seam weld strength (kN/m)
150	Cell wall height (mm)
400	Distance between weld seams (mm)
300 × 250	Cell dimension (mm)

In this research, geocell has been prepared from available thin and perforated geomembrane sheets with the ultimate tensile strength of 15 kN/m. This is small enough for better interaction with soil. Hegde and Sitharam (2015a, b, c) used geogrid with 20 kN/m ultimate tensile strength to prepare geocell. The engineering and geometry properties of manufactured geocell used in the current research are presented in Table 2.

4. Test procedure

In the present research work, all tests were performed on sand with two relative densities of 35% and 65%. Compaction technique was used in the test tank to achieve these densities using 4 and 15 blows of a 12 kg steel hammer as described by Lavasan and Ghazavi (2012). For each test, sand was initially poured in the box and compacted to reach 20 cm thick. To have a uniform relative density, the falling tamper was dropped from 60 cm height on a 50 cm × 50 cm steel plate with 5 mm thickness. Two relative densities were monitored and controlled by collecting samples in small aluminum cans with known volume placed at different locations in the test tank. The difference in densities measured at various locations was found to be less than 1.5%. The specific long ruler was used to level the soil surface in the test tank using numbered sings along the depth on the inside tank walls. For geocell-reinforced bed, these sings were used for sand filling to prescribed depths. Then geocell layer was placed on the top of the leveled sand and then cell pockets were filled with sand and continued to the prescribed footing bottom level.

When the supporting reinforced sandy bed was prepared, the footing plate was placed at the center of test tank beneath the center of the shaft jack. A load cell was oriented at the footing plate center. Then, dial gauges were placed on the footing and soil surfaces, as illustrated in Fig. 2. The load was applied using a hydraulic jack and maintained manually with an electric pump until the ultimate vertical deformation was reached. The loading procedure was performed according to ASTM-D1196M (2012), where the load increments were applied and maintained until the rate of settlement was less than 0.03 mm/min over three consecutive minutes. Each test took averagely 76 person-hour work.

5. Test program

The scheme of footing-soil system and instruments are shown in Fig. 2. Dimensionless parameters u/B , w/B , b/B , H/B , and h/B are used to describe test results. To save time and costs, some ratios including $b/B = 5$, $d/B = 0.44$ and $H/B = 0.3$ were kept constant in all tests. Also,

Table 3
Details of large scale test program.

Test series	Reinforcement type	N	u/B, h/B	w/B	D _r (%)	No. of tests
1	Unreinforced sand	–	–	–	35, 65	2 ^a + 1 ^b
2	FGR	1	0.1	0	35, 65	2 ^a + 1 ^b
3	GOR	1	0.1	0.92	35, 65	2 ^a + 1 ^b
4	GOR	1	0.1, 0.3, 0.54, 0.9	0.92	65	3 ^a + 1 ^b
5	GOR	1	0.1	0.92, 1.36, 1.84	65	2 ^a + 1 ^b
6	FGR and GOR	2	u/B = h/B = 0.1	0, 0.92	35	2 ^a

^a Number of main tests;

^b Number of Tests conducted for verification, repeatability and accuracy for test data.

b/B = 5 was considered based on findings of Sitharam and Sireesh (2005) and Hataf et al. (2010), who reached this optimum value. Dash et al. (2004) considered d/B = 1.2 and H/B = 2.75. It is noted that in the field, in general, footing width is greater than dimension of considered geocell. Therefore, in the current research, these ratios are closer to prototype conditions.

Six test series on footing supported by unreinforced sand, GOR and FGR methods were conducted, as outlined in Table 3. Test series 1 were carried out on unreinforced sand for reference purpose. Test series 2 were performed on FGR at two D_r values. Also, test series 3, 4 and 5 were carried out on GOR. To compare and understand the benefits of using of two geocell layers in FGR and GOR methods, test series 6 were carried out. Some tests were repeated to find out if test results are repeatable and indicative. The maximum differences between the bearing pressures at a given settlement ratio obtained from two trial tests were around 9% which shows that testing procedure is accurate and reliable.

6. Results and discussion

Normally the effect of soil reinforcement on the footing load-carrying characteristics is determined using the bearing capacity ratio, BCR, (DeMerchant et al., 2002; Dash et al., 2003; Sitharam and Sireesh, 2005; Demir et al., 2013; Lavasan and Ghazavi, 2012; Ghazavi and Lavasan, 2008). The footings supported on geosynthetics-reinforced soil normally do not show clear failure (Dash et al., 2001a,b). In small scale laboratory tests, the soil-footing system capacity is achieved at large footing settlements, sometimes up to 40–50% B (Dash et al., 2003), which makes no sense in practice. Hence, in this paper, to evaluate the reinforcement effect, a non-dimensional improvement factor, IF is defined. This value defines the ratio of bearing pressure of footing on geocell reinforced soil (q_{rein}) divided by that of the same footing on unreinforced soil (q_{unrein}) at a specified settlement, s_f . The values of 1%, 2%, 4%, 6%, 8%, 10%, 12%, 14%, 16%, 18%, and 20% are considered for s_f/B .

6.1. The general behavior of GOR and FGR

The bearing pressure versus settlement responses of the footing for unreinforced and geocell reinforced footings at two densities are shown in Fig. 3. As seen, by using FGR and GOR, the bearing pressure generally increases and the settlement decreases. Even at a large settlement, clear signs of failure were not evident in the case of geocell-reinforced foundations. Dash et al. (2001a) and Hegde and Sitharam (2015a, b) reported similar results for FGR on small-scale tests.

The value of IF at $s/B = 10\%$ for several studies that used geocell reinforced sand is presented in Table 4. In this research, considering the use of the factory produced geocell and the large size of loading plate, the ratios H/B and d/B are closer to the field conditions. Therefore, the results of this study can be extrapolated more accurately to full-scale

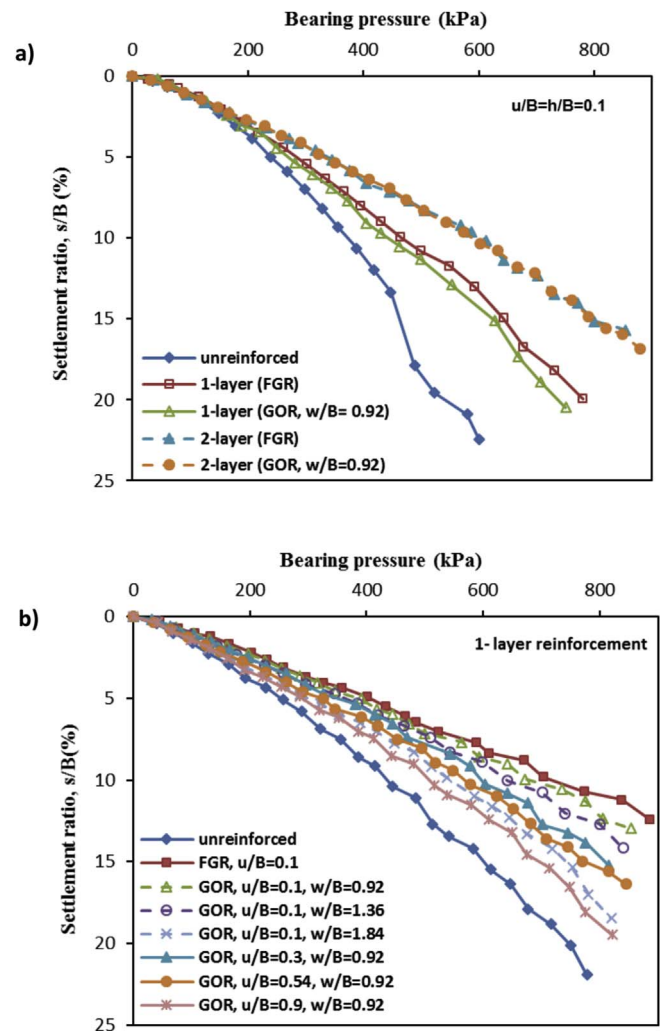


Fig. 3. Variation of footing bearing pressure versus settlement ratio for: (a) D_r = 35%; (b) D_r = 65%.

Table 4
Comparison of IF for footings on geocell reinforced sand at $s/B = 10\%$.

Reference	u/B	H/B	d/B	b/B	IF	Description
Dash et al. (2001a, b)	0.1	2.75	1.2	6	2.4	SP, D _r = 70%, F = 42.2°
Hegde and Sitharam (2015a, b, c)	0.1	1	1.21	5.9	1.28	SP, D _r = 65%, F = 36°
Present study	0.1	0.3	0.44	5	1.57	SP, D _r = 65%, F = 41°

cases.

Fig. 4 presents the variation of IF values with s/B for sand with D_r = 35% and D_r = 65%. Both Figs. 3 and 4 clearly show that the GOR with opening width equal to about the footing width ($w/B \sim 1$) improves the footing load-carrying response almost similar to FGR. As seen in Fig. 4, the maximum difference between IF values offered by one FGR layer and one GOR layer with $w/B = 0.92$ only accounts for about 6% and 8% for sand with D_r = 35% and 65%, respectively. This indicates that the use of one layer of GOR method with w/B up to 0.92 can have almost the same improvement as one FGR layer has. As also shown in Figs. 3a and 4a, two GOR layers with $w/B = 0.92$ give almost the same soil-footing system improvement as two FGR layers do.

Fig. 5 illustrates the variation of the soil heave at a distance of 1.5B from the center of the footing (δ_1) for two sand densities. As seen, the

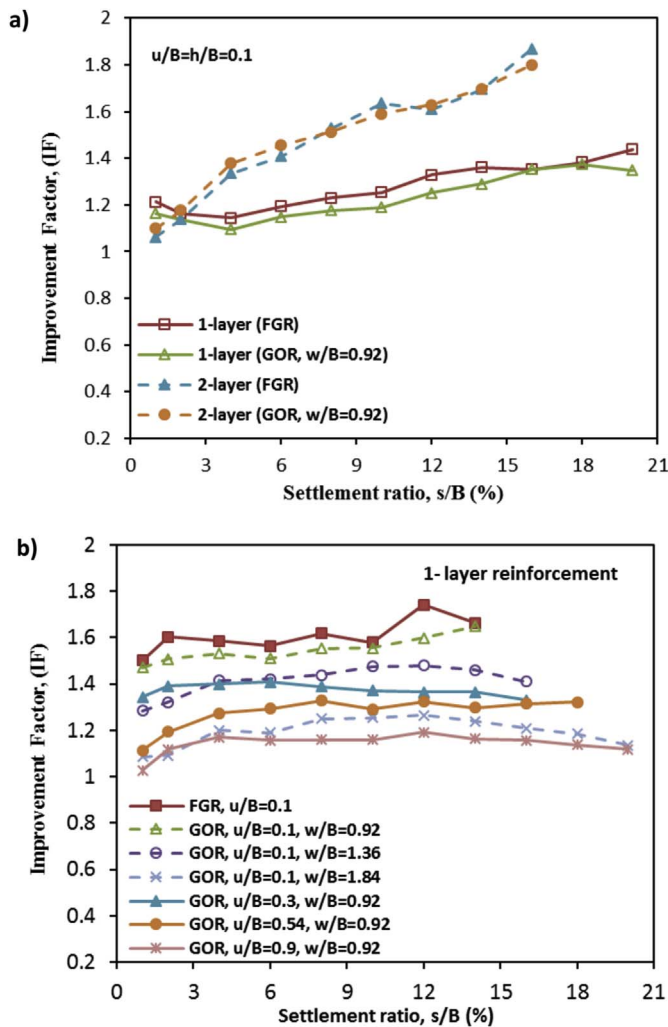


Fig. 4. Variation of IF values versus settlement ratio for: (a) $D_r = 35\%$; (b) $D_r = 65\%$.

use of geocell reinforcement decreases the heave values at various footing pressures. The maximum difference between heave ratio at 1.5B distance from the footing center ($\frac{\delta_1}{B}$) in one layer GOR with $w/B = 0.92$ and one layer FGR for sand with $D_r = 35\%$ and 0.65% are 4% and 16%, respectively. However, when two geocell layers are used, the heave is negligible for both GOR and FGR types (Fig. 5a).

The variation of the soil heave around the footing at 2.5B far from the footing center (δ_2) with bearing pressure is presented in Fig. 6. Both Figs. 5 and 6 clarify that the heave value at 1.5B from the footing center is significantly larger than that at 2.5B. This indicates that the footing loading has more influence at near distance zone compared to far distance zone.

6.2. Effect of depth of geocell reinforcement

To evaluate the effect of geocell mattress location from the footing bottom (u) on the footing bearing pressure and settlement, test series 4 were conducted. To avoid possible early buckling of geocell wall upon footing loading, $u/B = 0$ condition was not considered in tests. Fig. 7 shows the variation of footing bearing pressure with u/B for GOR with $w/B = 0.92$ in terms of various footing settlements. As seen, the footing bearing pressure decreases with increasing u/B up to almost $u/B = 0.3$, beyond which with further increasing u/B , the reinforcement effect decreases. Furthermore, at lower footing settlement, the effect of reinforcement location depth smoothly decreases. However, at greater s/B , the effect of u/B is more significant. The maximum reinforcement

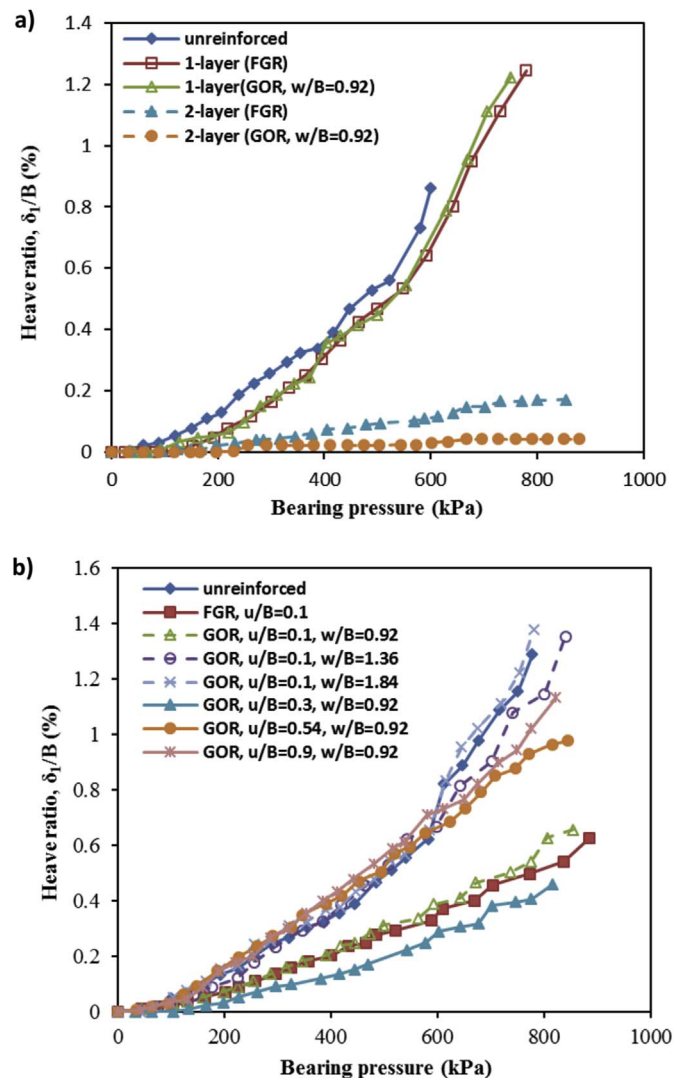


Fig. 5. Variation of $\frac{\delta_1}{B}$ with bearing pressure for: (a) $D_r = 35\%$; (b) $D_r = 65\%$.

improvement values for footing with $u/B = 0.1$ and $u/B = 0.9$ are 1.64 and 1.19, respectively (Fig. 4b), confirming that increasing the u/B values reduces IF values. In fact, for $u/B > 0.9$, the reinforcement effect vanishes and the sand bed performs like an unreinforced sand. This is because the footing applied pressure is distributed within the unreinforced soil mass above geocell mattress. Dash et al. (2001a,b) and Sitharam and Sireesh (2005) reported similar finding upon using full geocell reinforcement.

It is also necessary to note that with increasing u/B up to 0.3, the surface heave at 1.5B from the footing center decreases, whereas for $u/B > 0.3$, with increasing this value, the heave increases (Fig. 5b). This changes in trend of surface deformation with u/B of 0.3 maybe due to the soil mass encased between the footing bottom and geocell layer would be squeezed out, leading to lower stiffness under the footing applied pressure. However, for $u/B = 0.1$, the soil mass is more engaged and cannot move easily in the lateral directions. In addition, for $u/B = 0.3$, geocell mattress is in the most effective applied stress zone completely and the applied pressure is transferred to further distance within footing-geocell-soil block. For about $u/B = 0.9$, the surface heave value (δ_1) approaches that of unreinforced condition. The findings on the surface heave in the current paper have been confirmed by performing repeated tests. To the best knowledge of the authors, no heave deformations at different distances from footings on reinforced soil have been reported in the literature.

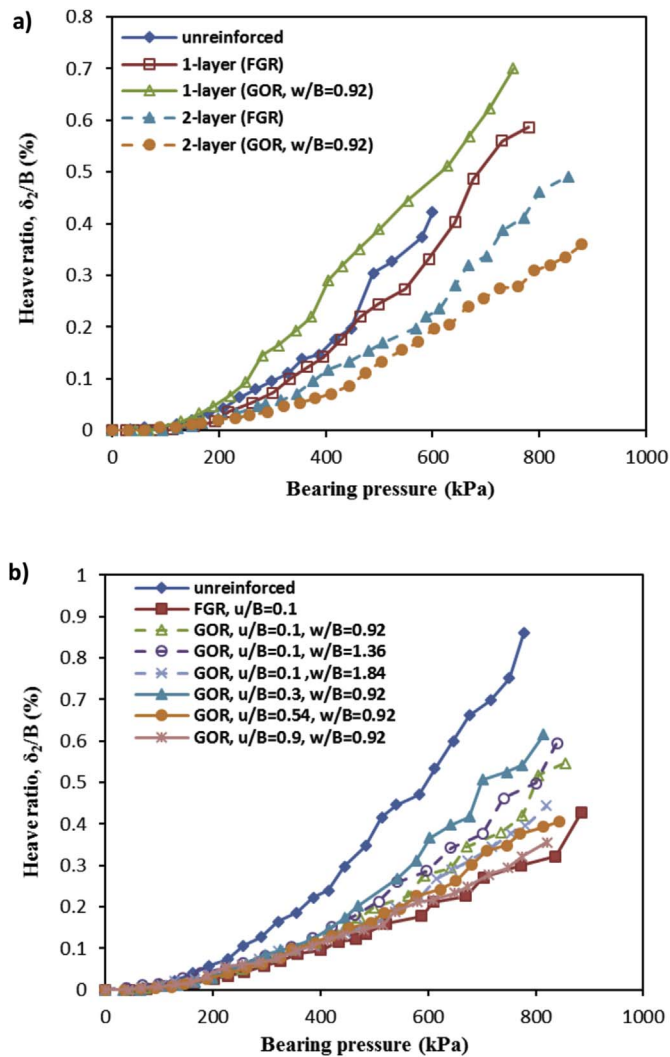


Fig. 6. Variation of δ_z/B with bearing pressure for (a) $D_r = 35\%$; (b) $D_r = 65\%$.

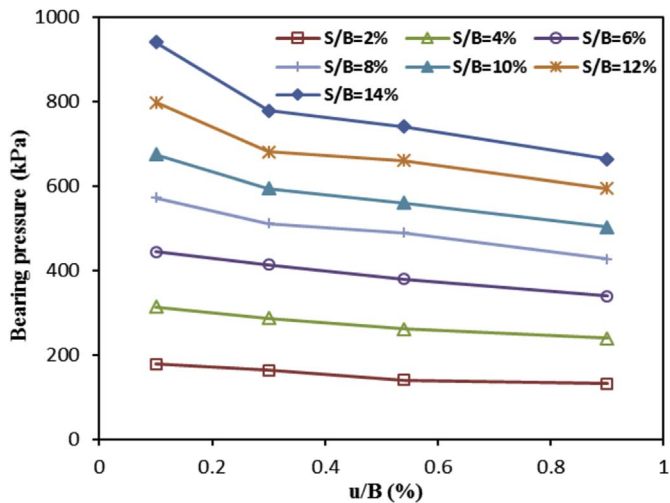


Fig. 7. Variation of footing bearing pressure versus u/B at various s/B for GOR with $N = 1$; $w/B = 0.92$; $D_r = 65\%$.

6.3. Effect of width of geocell with opening mattress

The influence of w/B on footing load-settlement characteristics was determined from test series 5. With increasing w/B at a specified

applied pressure on the footing, its settlement increases and at a given settlement, the footing tolerates lower pressure (Fig. 3b). In addition, Fig. 4b depicts that the maximum IF value decreases from 1.64 for $w/B = 0.92$ to 1.1 for $w/B = 1.84$. Figs. 3b and 4b show that up to $w/B = 0.92$, almost no reduction in the IF values occurs. Thus, for $w/B < 1$, no noticeable difference is observed between FGR and GOR effects. This difference accounts for about 8% for $w/B = 0.92$.

Fig. 5b illustrates that with increasing w/B , the soil heave at $1.5B$ from the footing center increases. With increasing w/B up to around 0.92, almost no differences between geocell with opening and full geocell reinforcement are observed on surface heave at $1.5B$. With increasing w/B beyond 0.92, the soil surface heave increases and geocell reinforced-sand bed has a similar response to unreinforced one. This is because for $w/B > 0.92$, the stiffness of the reinforced sand bed decreases and reinforced layer cannot transfer the applied pressure to deeper zones. As a result, like unreinforced case, the surface heave increases.

Fig. 6b shows that with increasing w/B , the value of δ_{2L} increases, however, its variation with the footing bearing pressure is less than δ_1 . This proves that the influence of footing bearing pressure at far distance ($2.5B$) from the footing center is less than that at near distance ($1.5B$). The maximum difference for δ_{2L} between FGR and GOR with $w/B = 1.36$ occurs. For $w/B > 1.36$, the surface heave δ_{2L} starts to decrease. For example, for $w/B = 1.84$, the surface heave δ_{2L} is less than that for $w/B = 1.36$ (Fig. 6b). The reason is that for $w/B > 1.36$, there exists lower stiffness beneath the footing and thus geocell mattress cannot spread the applied pressure over an extended area. Therefore, like unreinforced bed, most deformations occur near the footing bottom.

Given that, changes in opening width in geocell layer (GOR) affects failure mechanism and maximum surface deformation occurs at various distances from the footing, it may not possible to make a judgement on improvement of soil surface deformation by comparison of heave at two particular points. To compare the improvement of surface deformation, it is required to measure surface deformation at various distances continuously.

6.4. Effect of soil relative density

Test series 1, 2 and 3 were performed to investigate the behavior of the footing on unreinforced, FGR and GOR types for sand with $D_r = 35\%$ and 65% . Fig. 4 shows that IF values for one layer FGR with $D_r = 35\%$ and 65% are 1.43 and 1.74, respectively. For one layer GOR with $w/B = 0.92$, these values are 1.37 and 1.64 for sand with $D_r = 35\%$ and 65% , respectively. In general, both bearing pressure and settlement of the footing for FGR and GOR methods are more improved for more compacted sand. Dash et al. (2001a, b) reported similar results for FGR.

The geocell reinforced bed can enhance footing performance by providing lateral and vertical confinement, tensioned membrane effect and wider stress distribution. According to Pokharel et al. (2010), due to the three-dimensional structure of geocell, it provides lateral confinement to soil particles within its cells. In sand with greater relative density, sand grains dilate and thus greater strains will be mobilized in the geocell layer. This causes lateral confinement increases. The geocell provides vertical confinement in two ways. First, the friction between the infill material and the geocell wall. Second, the geocell-reinforced base acts as a mattress to restrain the soil from moving upward outside the loading area. In more compacted sand, the interface friction angle of geocell wall-sand increases. Accordingly, vertical confinement in both ways increases. The tensioned membrane or beam effect is referred as the tension developed in curved geocell-reinforced mattress to resist the vertical load (Rajagopal et al., 1999). The increased relative density of sand makes geocell reinforced section stiffer. Hence, the curved surface exerts a greater upward reaction and reduces further net stress applied to soil bed. In more compacted sand, because of greater

rigidity of geocell layer, the footing pressure distributes over a wider area and pressure transmitted to the soil decreases, leading to an improvement in the footing performance. All effects mentioned above increase further footing performance at higher density for both FGR and GOR methods. In GOR, each effect may have different intensity compared to in FGR. For example, lateral confinement in GOR due to openings beneath the footing may have lower intensity than in FGR. Also, second way of vertical confinement may be more significant than other effects. This is because geocell layer for GOR is outside the loading area like FGR is complete and it can restrain the soil from moving upward. It should be noted that, the study adopts an experimental approach and complete understanding of failure mechanisms requires comprehensive numerical and analytical efforts.

Fig. 5 shows that unlike unreinforced sand bed, at 1.5B distance from the footing center, the surface heave is different for geocell reinforced sand with $D_r = 35\%$ and 65% . For GOR with $w/B = 0.92$, at 750 kPa footing pressure, δ_1 decreases about 130% for $D_r = 65\%$ compared with that due to $D_r = 35\%$. This is because the footing pressure is distributed over a much larger area due to the rigidity of geocell layer in dense sand bed.

6.5. Effect of the number of geocell layers

Test series 6 were carried out on two GOR and FGR layers. Figs. 3a and 4a show that the IF value increases with increasing N from 1 to 2 for both FGR and GOR types due to providing stiffer bed. The maximum difference in IF values at a given footing settlement for $N = 2$ layers in FGR and GOR with $w/B = 0.92$ is about 2%. For $N = 1$, this difference accounts for about 7%. This indicates that with an increase in number of layers of geocell, the influence of opening in reinforcement decreases.

Figs. 5a and 6a show that with increasing N from 1 to 2, the surface heave (δ_1 , δ_2) decreases considerably. For example, when two geocell layers in FGR and GOR types ($w/B = 0.92$) are used, at 750 kPa footing pressure, δ_1 decreases about 86% and 96%, respectively, compared with one layer reinforcement cases. The probable reason for heave reduction is that the use of two geocell layers increases flexural stiffness of reinforced bed and it can re-distribute the stresses into deeper zones. Consequently, less passive resistance is produced and surface deformation decreases.

7. Scale effect

According to dependence of 1-g tests on scale, their results may not directly applicable to the prototype case. Considering large dimensions of the model footing with $B = 50$ cm, using real geocell in this paper and since some real footings are close to this range of dimension, the results may be applied for the same range of footings. As suggested by Fakhri and Jones (1996), the results of small scale model tests can be extrapolated to prototype cases by carefully applying the scaling laws. Considering the width of prototype plate will be N times higher than the model plate,

$$\frac{B_p}{B_m} = N \quad (1)$$

where N is the scaling factor; B_m is footing width in the model; B_p is footing width in prototype.

A dimensional analysis can be used to deduce the scaling laws involving the relationship between the parameters that could affect the case which is being modeled. The theory of dimensional analysis was explained in detail by Buckingham (1914).

Based on equations obtained from dimensional analysis by Hegde and Sitharam (2015b):

$$\frac{K_{g(p)}}{K_{g(m)}} = N^2 \quad (2)$$

where $k_{g(m)}$ and $k_{g(p)}$ refer to tensile strength of the model and prototype geocell material, respectively. Since tensile strength of the geocell used in this study equals 15 kN/m and maximum tensile strength of geocells available in market is about 30 kN/m, based on the Eq. (2):

$$\frac{K_{g(p)}}{K_{g(m)}} = \frac{30}{15} = N^2 = 2 \quad (3)$$

Hence, the scaling factor (N) can be calculated as $\sqrt{2}$.

Using geocell with tensile strength of 30 kN/m and considering geometrical scale in practice, the results obtained by the model can be applied for a footing 70.7 cm ($50 \text{ cm} \times \sqrt{2}$) in length. Fakhri and Jones (1996) warned that, it is not feasible to use complete similarity between model and prototype due to involvement of several complex factors. They stated that it should be left to the judgment of the researchers to decide about the factors to scale up considering the accuracy and the nature of the problem.

8. Limitations and applicability

In the current research, the results obtained for load-settlement response of footings supported by geocell-reinforced sand with two forms of FGR and GOR are interesting, especially due to using large model footings. A new idea called GOR has been presented which may be used in practice to improve load-settlement of footings on geocell-reinforced soil. The GOR method may be used practically prior to the footing construction. Also, in some already constructed footings, the access to the footing bottom level is impossible or difficult. In addition, in some cases, where excavation beneath the footings for reinforcement is time-consuming, reinforcement operations beneath the footing lead to postpone the foundation construction. Thus, the GOR method makes foundation construction independent of implementation of reinforcement operations. For this purpose, the soil close to the footing edge may be cautiously excavated, then geocell layer is spread and then, filled with soil. Foundation reinforcement can be accomplished step by step for safety. The latter is just a recommendation and the authors did not perform their tests in this manner. Therefore, this application is left for further investigation. The presented results are helpful to understand the basic mechanism and overall trends in the results of GOR method. Centrifuge model tests or full-scale model tests are recommended to ascertain the findings.

In this research, due to difficulties associated with test procedure preparation, time-consumption in conducting tests, providing homogeneous soil bed, size limitation of the test tank and costs involved, the obtained results are based on considered geocell type, pocket size of geocell, height of geocell, foundation width, sand type, sand compaction, soil grain size distribution, footing size, footing shape, plate stiffness, tensile strength of geocell wall sheets, footing applied pressure, test preparation method, etc. Therefore, further studies are recommended to consider the influence of other values of these variables on the results.

9. Conclusions

A new idea has been presented in this paper to investigate the behavior of footing supported on geocell-reinforced sand by performing tests on 500 mm × 500 mm steel plate as footing. For this purpose, geocell with opening (GOR) and full geocell (FGR) layer/layers has/have been used for sand reinforcement. In addition, as a new contribution, the soil surface heave was also measured simultaneously at close and far distances from the footing. The influence of location depth, opening width, number of geocell layers and soil relative density with FGR and GOR types has been investigated. The main concluding remarks may be summarized as:

- In general, using GOR (with opening) like FGR (full geocell) improves pressure-settlement characteristics of footings. The load-

carrying behavior of footing on GOR layer/layers with $w = 0.92B$ is almost similar to that of the footing on FGR mattress. The maximum difference between bearing capacity improvement of two reinforcement types is limited to 6%–8% for one reinforcement layer. Thus, this type of footing soil reinforcement is beneficial and economical in practical applications.

- For FGR and GOR types, the bearing pressure decreases at a given settlement with increasing the placement depth of geocell layer from the footing bottom. For GOR type descending trend of bearing pressure in placement depth beyond $u/B = 0.3$ decreases. Beyond $u/B = 0.9$, the behavior of reinforced bed becomes similar to that of unreinforced sand bed.
- At a given footing pressure, the footing settlement increases with increasing w/B in GOR type. In addition, for $w/B < 0.92$, there is no a considerable difference between reinforcement effect of FGR and GOR on the soil surface heave at near (1.5B) or far (2.5B) distances from the footing center.
- With increasing the soil relative density and the number of geocell layers from $N = 1$ to 2 in both FGR and GOR types, the footing bearing pressure increases, the settlement decreases, and the soil surface heave decreases.

References

- Adams, M.T., Collin, J.G., 1997. Large model spread footing load tests on geosynthetic reinforced soil foundations. *J. Geotech. Geoenviron. Eng.* ASCE 123 (1), 66–72.
- ASTM D1196M, 2012. Standard Test Method for Nonrepetitive Static Plate Load Tests of Soils and Flexible Pavement Components, for Use in Evaluation and Design of Airport and Highway Pavements. ASTM International, West Conshohocken, PA, USA.
- Badakhshan, E., Noorzad, A., 2017. Effect of footing shape and load eccentricity on behavior of geosynthetic reinforced sand bed. *Geotext. Geomembr* 45 (2), 58–67.
- Biabani, M.M., Indraratna, B., Ngo, T.N., 2016. Modelling of geocell-reinforced subballast subjected to cyclic loading. *Geotext. Geomembr* 44 (4), 489–503.
- Binquet, J., Lee, K.L., 1975. Bearing capacity tests on reinforced earth slabs. *J. Geotech. Eng. Div., ASCE* 101 (12), 1241–1255.
- Biswas, A., Krishna, A.M., Dash, S.K., 2013. Influence of subgrade strength on the performance of geocell-reinforced foundation systems. *Geosynth. Int.* 20 (6), 376–388.
- Boushehrian, A.H., Hataf, N., Ghahramani, A., 2011. Modeling of the cyclic behavior of shallow foundations resting on geomesh and grid-anchor reinforced sand. *Geotext. Geomembr* 29 (3), 242–248.
- Buckingham, E., 1914. On physically similar systems; illustrations of the use of dimensional equations. *Phys. Rev.* 4 (4), 345–376.
- Bush, D.I., Jenner, C.G., Basset, R.H., 1990. The design and construction of geocell foundation mattress supporting embankments over soft ground. *Geotext. Geomembr* 9 (1), 83–98.
- Chen, R.H., Huang, Y.W., Huang, F.C., 2013. Confinement effect of geocells on sand samples under triaxial compression. *Geotext. Geomembr* 37 (2), 35–44.
- Chung, W., Cascante, G., 2007. Experimental and numerical study of soil-reinforcement effects on the low-strain stiffness and bearing capacity of shallow foundations. *Geotech. Geol. Eng.* 25, 265–281.
- Dash, S.K., Krishnaswamy, N.R., Rajagopal, K., 2001a. Bearing capacity of strip footings supported on geocell-reinforced sand. *Geotext. Geomembr* 19 (4), 235–256.
- Dash, S.K., Rajagopal, K., Krishnaswamy, N.R., 2001b. Strip footing on geocell reinforced sand beds with additional planar reinforcement. *Geotext. Geomembr* 19 (8), 529–538.
- Dash, S.K., Sireesh, S., Sitharam, T.G., 2003. Model studies on circular footing supported on geocell reinforced sand underlain by soft clay. *Geotext. Geomembr* 21 (4), 197–219.
- Dash, S.K., Rajagopal, K., Krishnaswamy, N.R., 2004. Performance of different geosynthetic reinforcement materials in sand foundations. *Geosynth. Int.* 11 (1), 35–42.
- Dash, S.K., Rajagopal, K., Krishnaswamy, N.R., 2007. Behaviour of geocell reinforced and beds under strip loading. *Can. Geotech. J.* 44 (7), 905–916.
- Dash, S.K., 2012. Effect of geocell type on load-carrying mechanisms of geocell-reinforced sand foundations. *Int. J. GeoMech.* 12 (5), 537–548.
- Demir, A., Laman, M., Yildiz, A., Ornek, M., 2013. Large scale field tests on geogrid reinforced granular fill underlain by soft clay. *Geotext. Geomembr* 38 (1), 1–15.
- DeMerchant, M.R., Valsangkar, A.J., Schriver, A.B., 2002. Plate load tests on geogrid reinforced expanded shale lightweight aggregate. *Geotext. Geomembr* 20 (3), 173–190.
- El Sawwaf, M.A., 2007. Behaviour of strip footing on geogrid-reinforced sand over a soft clay slope. *Geotext. Geomembr* 25 (1), 50–60.
- Fakher, A., Jones, C.J.F.P., 1996. Discussion on bearing capacity of rectangular footings on geogrid reinforced sand. by Yetimoglu, T., Wu, J.T.H., Saglam, A., 1994. *J. Geotech. Eng.* 122, 326–327.
- Fragaszy, R.J., Lawton, E., 1984. Bearing capacity of reinforced sand subgrades. *J. Geotech. Eng.* 110 (10), 1500–1507.
- Ghazavi, M., Lavasan, A.A., 2008. Interference effect of shallow foundations constructed on sand reinforced with geosynthetics. *Geotext. Geomembr* 26 (5), 404–415.
- Ghosh, A., Ghosh, A., Bera, A.K., 2005. Bearing capacity of square footing on pond ash reinforced with jute-geotextile. *Geotext. Geomembr* 23 (2), 144–173.
- Hataf, N., Boushehrian, A.H., Ghahramani, A., 2010. Experimental and numerical behavior of shallow foundations on sand reinforced with geogrid and grid-anchor under cyclic loading. *Sci. Iran. Trans. A-Civ. Eng.* 17 (1), 1–10.
- Hegde, A., Sitharam, T.G., 2015a. 3-dimensional numerical modelling geocell reinforced sand beds. *Geotext. Geomembr* 43, 171–181.
- Hegde, A., Sitharam, T.G., 2015b. Experimental and numerical studies on protection of buried pipelines and underground utilities using geocells. *Geotext. Geomembr* 43 (5), 372–381.
- Hegde, A., Sitharam, T.G., 2015c. Use of bamboo in soft ground engineering and its performance comparison with geosynthetics: experimental studies. *J. Mater. Civ. Eng.* 27 (9), 1–9.
- Hegde, A., Sitharam, T.G., 2017. Experiment and 3D-numerical studies on soft clay bed reinforced with different types of cellular confinement systems. *Transp. Geotech* 10, 73–84.
- Kargar, M., Mir Mohammad Hosseini, S.M., 2017. Effect of reinforcement geometry on the performance of a reduced-scale strip footing model supported on geocell-reinforced sand. *Sci. Iran. Trans. A-Civ. Eng.* 24 (1), 96–109.
- Khing, K.H., Das, B.M., Puri, V.K., Cook, E.E., Yen, S.C., 1993. The bearing capacity of a strip foundation on geogrid reinforced sand. *Geotext. Geomembr* 12 (4), 351–361.
- Koerner, R.M., 2012. sixth ed. Designing with Geosynthetics, vol. 1 Xlibris Corporation, USA.
- Kusakabe, O., 1995. In: Taylor, R.N. (Ed.), Chapter 6: Foundations. *Geotechnical Centrifuge Technology*. Blackie Academic & Professional, London, pp. 118–167.
- Latha, G.M., Somwanshi, A., 2009. Bearing capacity of square footings on geosynthetic reinforced sand. *Geotext. Geomembr* 27 (4), 281–294.
- Lavasan, A.A., Ghazavi, M., 2012. Behavior of closely spaced square and circular footings on reinforced sand. *Soils Found.* 52 (1), 160–167.
- Lavasan, A., Ghazavi, M., Schanz, T., 2017. Analysis of interfering circular footings on reinforced soil by physical and numerical approaches considering strain dependent stiffness. *Int. J. Geomech.* [https://doi.org/10.1061/\(ASCE\)GM.1943-5622.0000992](https://doi.org/10.1061/(ASCE)GM.1943-5622.0000992).
- Ngo, N.T., Indraratna, B., Rujikiatkamjorn, C., Biabani, M.M., 2016. Experimental and discrete element modeling of geocell-stabilized subballast subjected to cyclic loading. *J. Geotech. Geoenviron. Eng., ASCE* 142 (4) 04015100–04015100-04015100-14.
- Oliaei, M., Kouzegaran, S., 2017. Efficiency of cellular geosynthetics for foundation reinforcement. *Geotext. Geomembr* 45 (2), 11–22.
- Pokharel, S.K., Han, J., Leshchinsky, D., Parsons, R.L., Lahalmi, I., 2010. Investigation of factors influencing behavior of single geocell reinforced bases under static loading. *Geotext. Geomembr* 28 (6), 570–578.
- Rajagopal, K., Krishnaswamy, N.R., Madhavi Latha, G., 1999. Behaviour of sand confined with single and multiple geocells. *Geotext. Geomembr* 17, 171–181.
- Rea, C., Mitchell, J.K., 1978. Sand Reinforcement Using Paper Grid Cells. ASCE Spring Convention and Exhibit, Pittsburgh, PA, April, 24–28, Preprint 3130.
- Roy, S.S., Deb, K., 2017. Effects of aspect ratio of footings on bearing capacity for geogrid-reinforced sand over soft soil. *Geosynth. Int.* 24 (4), 362–382.
- Sharma, R., Chen, Q., Abu-Farsakh, M., Yoon, S., 2009. Analytical modeling of geogrid reinforced soil foundation. *Geotext. Geomembr* 27 (1), 63–72.
- Sitharam, T.G., Sireesh, S., 2005. Behavior of embedded footings supported on geogrid cell reinforced foundation beds. *Geotech. Test J.* 28 (5), 452–463.
- Sitharam, T.G., Hegde, A., 2013. Design and construction of geocell foundation to support the embankment on settled red mud. *Geotext. Geomembr* 41, 55–63.
- Shahin, H.M., Nakai, T., Morikawa, Y., Masuda, S., Mio, S., 2017. Effective use of geosynthetics to increase bearing capacity of shallow foundations. *Can. Geotech. J.* 54 (12), 1647–1658.
- Shimizu, M., Inui, T., 1990. Increase in the bearing capacity of ground with geotextile wall frame. In: Proceedings of Fourth International Conference on Geotextiles Geomembranes and Related Products, Vol. 1. Hague, Netherlands, 254.
- Ueno, K., Miura, K., Maeda, Y., 1998. Prediction of ultimate bearing capacity of surface footings with regard to size effects. *Soils Found.* 38 (3), 165–178.
- Yoon, Y.W., Cheon, S.H., Kang, D.S., 2004. Bearing capacity and settlement of tire-reinforced sands. *Geotext. Geomembr* 22 (5), 439–453.